

Yale University

EliScholar – A Digital Platform for Scholarly Publishing at Yale

Yale Medicine Thesis Digital Library

School of Medicine

1-1-2019

Identifying Quantitative Enhancement-Based Imaging Biomarkers In Patients With Colorectal Cancer Liver Metastases Undergoing Loco-Regional Tumor Therapy

Mansur Abdul Ghani

Follow this and additional works at: <https://elischolar.library.yale.edu/ymtdl>



Part of the [Medicine and Health Sciences Commons](#)

Recommended Citation

Ghani, Mansur Abdul, "Identifying Quantitative Enhancement-Based Imaging Biomarkers In Patients With Colorectal Cancer Liver Metastases Undergoing Loco-Regional Tumor Therapy" (2019). *Yale Medicine Thesis Digital Library*. 3497.

<https://elischolar.library.yale.edu/ymtdl/3497>

This Open Access Thesis is brought to you for free and open access by the School of Medicine at EliScholar – A Digital Platform for Scholarly Publishing at Yale. It has been accepted for inclusion in Yale Medicine Thesis Digital Library by an authorized administrator of EliScholar – A Digital Platform for Scholarly Publishing at Yale. For more information, please contact elischolar@yale.edu.

**Identifying Quantitative Enhancement-based Imaging Biomarkers in Patients with
Colorectal Cancer Liver Metastases undergoing Loco-regional Tumor Therapy**

A Thesis Submitted to the Yale University School of Medicine
in Partial Fulfillment of the Requirements for
the Degree of Doctor of Medicine

by

Mansur Abdul Ghani

2019

Identifying Quantitative Enhancement-based Imaging Biomarkers in Patients with Colorectal Cancer Liver Metastases undergoing Loco-regional Tumor Therapy

Mansur A. Ghani, Julius Chapiro, and Todd Schlachter. Section of Interventional Radiology, Department of Radiology and Biomedical Imaging, Yale School of Medicine, New Haven, CT

The purpose of this study was to test and compare the ability of radiologic measurements of lesion diameter, volume, and enhancement on baseline magnetic resonance (MR) images to be predictors of overall survival (OS) and markers of treatment response in patients with liver-dominant colorectal cancer metastases undergoing loco-regional tumor therapies.

This retrospective study included 88 patients with colorectal cancer (CRC) liver metastases, treated with transarterial chemoembolization (TACE) or Y90 transarterial radioembolization (TARE) between 2001 and 2014. All patients received contrast-enhanced MRI prior to therapy. Semi-automated whole liver and tumor segmentations of three dominant lesions were performed on baseline MRI to calculate total tumor volume (TTV) and total liver volumes (TLV). Quantitative 3D analysis was performed to calculate enhancing tumor volume (ETV), enhancing tumor burden (ETB, calculated as ETV/TLV), enhancing liver volume (ELV), and enhancing liver burden (ELB, calculated as ELV/TLV). Overall and enhancing tumor diameters were also measured. Response assessment was analyzed in a subset of 63 patients who received 1-month MRI follow-up imaging using RECIST, mRECIST, change in ELV (Δ ELV), vRECIST and qEASL. A modified Kaplan-Meier method was used to determine appropriate cutoff values to stratify patients based on these metrics. The predictive value of each parameter was assessed by Kaplan-Meier survival curves as well as univariate and multivariate cox proportional hazard models (statistical significance defined as $p < .05$).

In baseline imaging analysis, all methods except ELB achieved statistically significant separation of survival curves. Multivariate analysis showed a HR of 2.1 (95% CI 1.3-3.4, $p=0.004$) for enhancing tumor diameter, HR 1.7 (95% CI 1.1-2.8, $p=0.04$) for TTV, HR 2.3 (95% CI 1.4-3.9, $p<0.001$) for ETV, and HR 2.4 (95% CI 1.4-4.0, $p=0.001$) for ETB. Among treatment response assessment methods, only vRECIST achieved statistically significant separation of survival curves and gave a HR of 2.1 (95% CI 1.1-4.0, $p=0.02$).

In conclusion, tumor enhancement of CRC liver metastases on baseline MR imaging is strongly associated with patient survival after loco-regional tumor therapy, suggesting that ETV and ETB are better prognostic indicators than non-enhancement based and one-dimensional based markers. However, while volumetric-based methods are superior to 1D methods, enhancement-based methods of treatment response assessment were not successful in predicting survival. A potential implication of these findings as novel staging markers warrants prospective validation.

Acknowledgements

I greatly appreciate the Yale School of Medicine Office of Student Research and the Radiological Society of North America for their generous funding of this research.

I am incredibly grateful to Dr. Todd Schlachter and Dr. Julius Chapiro for making this thesis possible, and going above and beyond the obligations of good mentors. Under their tutelage and guidance, the Yale Interventional Oncology Research Lab has become another family to me that has fostered all areas of my professional and personal growth.

Thank you to my parents, Shahid Ghani and Arshia Rahman for their unconditional love and support. I owe any and every success I achieve in my life to your sacrifices. To my brother, Yusuf Ghani, thank you for always reminding me what really matters in life. Finally, to my best friend and beautiful wife, Naureen Rashid, thank you for being the greatest companion I could ask for, and I can't wait to experience all of life's adventures with you.

Table of Contents

INTRODUCTION.....	1
METHODS.....	5
RESULTS PART I: BASELINE MR IMAGING ANALYSIS.....	15
RESULTS PART II: TREATMENT RESPONSE ASSESSMENT	25
DISCUSSION	37
REFERENCES.....	42

Introduction

Colorectal cancer (CRC) is the third most common cancer in the world and the second leading cause of cancer-related deaths worldwide, resulting in 700,000 deaths per year (1). The mortality rate from CRC has dropped over the last several decades due to increased screening and prevention as well as more effective treatment options; the 1-year and 5-year survival of patients with CRC have improved to 83.2 and 64.3% respectively. However, the occurrence of CRC metastases to distant organs drops the 5-year survival to 11.7% (2). The liver is the most common site of metastatic disease, present in approximately 25% of patients at diagnosis with a prevalence of nearly 65% during the course of disease (3). Although surgical resection of the primary tumor and liver metastases is currently the most effective treatment option, this is generally feasible if there are ≤ 5 metastases per liver lobe, at least two adjacent tumor-free segments, and a liver remnant after surgery $>20\%$ (4). Only 10 to 25% of patients with hepatic metastases from CRC are candidates for hepatic resection at diagnosis (5). The remainder are treated with systemic chemotherapy with the goal of improving survival and, in some, downsizing to allow for liver resection (6). However, this is unable to prevent the development of progressive disease in the majority of patients (7). As a result, liver-directed loco-regional treatments for patients with unresectable hepatic metastases, in the form of image-guided intra-arterial therapies (IAT), including yttrium-90 (^{90}Y) transarterial radioembolization (TARE), conventional transarterial chemoembolization (cTACE), or drug-eluting bead TACE (DEB-TACE), are often indicated for palliative therapy (8–10).

Current guidelines by the National Comprehensive Cancer Network (NCCN) recommend that IATs may be used in patients with liver dominant metastatic disease ($\geq 80\%$ of tumor burden located in the liver) and when the level of hepatic involvement is not greater than 60% (11). Compared with systemic therapies, IATs can result in significantly higher concentrations of drugs within the tumor as well as a lower incidence of systemic toxicities and adverse events (12). In general, IATs mitigate drug toxicity and yield more robust local tumor control by targeting the mostly arterially supplied tumor tissue while sparing non-tumoral liver parenchyma, which is mainly fed through the portal vein (13). Three common IATs include cTACE, DEB-TACE and TARE. Conventional TACE delivers an emulsion of conventional chemotherapeutic agents carried by Lipiodol to the tumor-feeding artery. Lipiodol is an iodinated poppy seed oil-based medium that works as an effective drug carrier, partial embolic agent and contrast agent which is easily visualized under fluoroscopy and computed tomography (CT), helping to confirm targeting and complete tumor coverage (14). Polymer-based drug-eluting beads (DEBs) were developed with the hopes of delivering higher concentrations of chemotherapy to the tumor while improving systemic toxicities caused by cTACE (15). DEB-TACE results in a controlled release of chemotherapeutics over several hours to days after injection (16). TARE involves delivery to the tumor of radioactive microspheres that emit β -radiation into the surrounding tissue. It is also a safe and effective treatment for unresectable, chemorefractory colorectal cancer metastases to the liver (17).

The success of IATs in clinical trials has firmly established these interventional techniques as mainstays in palliative therapy for advanced hepatic metastatic disease, and

research efforts to improve the efficacy of these modalities continue to grow. However, currently there is no agreed upon prognostic staging system that can give accurate prognostic information regarding patients with advanced CRC (18). A number of studies have proposed classification and staging systems based on a variety of variables including the number of metastatic nodules, size of metastases, unilobar versus bilobar involvement, the extent of liver involvement, performance status, and serum alkaline phosphatase, but none of these systems have gained universal acceptance (19–23).

Instead, much current work has centered on the accurate assessment of treatment response. The primary clinical purpose of follow-up imaging is to be able to determine responders and non-responders with the purpose of informing therapeutic decisions. Several standard guidelines have been established to evaluate tumor morphology for this purpose. The two most common protocols are Response Evaluation Criteria in Solid Tumors (RECIST) and World Health Organization (WHO) criteria, which measure tumor diameters in one and two dimensions, respectively (24). However, these measures are poor indicators of response following IATs, as these procedures usually rely on embolization of tumor-feeding arteries resulting in necrosis of the tumor without immediate effects on overall size (25).

Due to this shortcoming, modified RECIST (mRECIST) and European Association for the Study of the Liver (EASL) criteria, which measure enhancing tumor diameter on contrast-enhanced MRI in one dimension or two dimensions, respectively, were developed. However, these 1D and 2D image assessment techniques are susceptible to inherent inaccuracies, including limited reproducibility and inability to quantify heterogeneous tumors (26). As a result, three-dimensional quantitative image analysis

techniques including volumetric RECIST (vRECIST) and quantitative EASL (qEASL) have been developed to more accurately quantify tumor response via volumetric tumor measurements and enhancing tumor volume (27). Preliminary studies have demonstrated the superiority of these techniques in predicting survival after intra-arterial therapy (28–30). Two recent studies determined that baseline 3D enhancement-based tumor burden analysis in hepatocellular carcinoma (HCC) patients better predicted survival than diameter- and non-enhancement-based measurements (31,32).

While assessment of treatment response is certainly beneficial in helping guide therapeutic decision-making, it may take anywhere from one to six months after the first IAT session to determine response depending on what assessment guidelines are used. A prognostic staging system is advantageous in its ability to inform clinical decision-making at the time of diagnosis. Tumor enhancement on imaging may be an important component of such a staging system. However, to date, no studies have investigated 3D enhancement-based analysis in CRC liver metastases prior to TACE or TARE. Additionally, there is a desirability to utilize a whole-liver approach to quantitative response. Currently available means of quantitating tumor enhancement requires segmentation of the tumor to delineate tumor borders from normal liver parenchyma. This can be a time-intensive process and the accuracy varies with the expertise of the operator. A whole-liver approach, on the other hand, quantitates the enhancement in the entire liver volume. This method only requires segmentation of the whole liver, which is much faster to generate, eliminates the subjectivity associated with lesion-based analysis, and accounts for tumor heterogeneity (29). It is important to address these gaps in knowledge to validate the use of 3D quantitative imaging techniques as indicators of

therapeutic efficacy in an increasing number of clinical trials and to inform clinical treatment recommendations for patients with hepatic metastases of CRC.

The purpose of our study was to (1) determine whether 3D whole-liver and tumor enhancement features can serve as a staging biomarker in patients with CRC metastases to the liver and (2) determine if a whole-liver approach can be used to measure treatment response.

Methods

Study cohort

This single-institution study was conducted in compliance with the Health Insurance Portability and Accountability Act and approved by the institutional review board. Between 2001 and December 2014, a total of 126 patients with liver-only or liver-dominant metastatic colorectal cancer (mCRC) underwent their first session of IAT within our institution and received contrast-enhanced MR imaging within 60 days following IAT. Patients were excluded if their baseline imaging was missing from the database (N=20). Additional patients were excluded if imaging was truncated or poor quality (e.g., motion artifact) (N=17). One patient was excluded because of failure of registration between the pre-and post-contrast images. The remaining 88 patients, treated with cTACE, DEB-TACE, or TARE, were included in the final analysis.

Of these 88 patients, 70 received one month post-procedure follow-up MR imaging. Seven were missing imaging from our patient database, resulting in 63 patients included for follow-up analysis (Fig. 1).

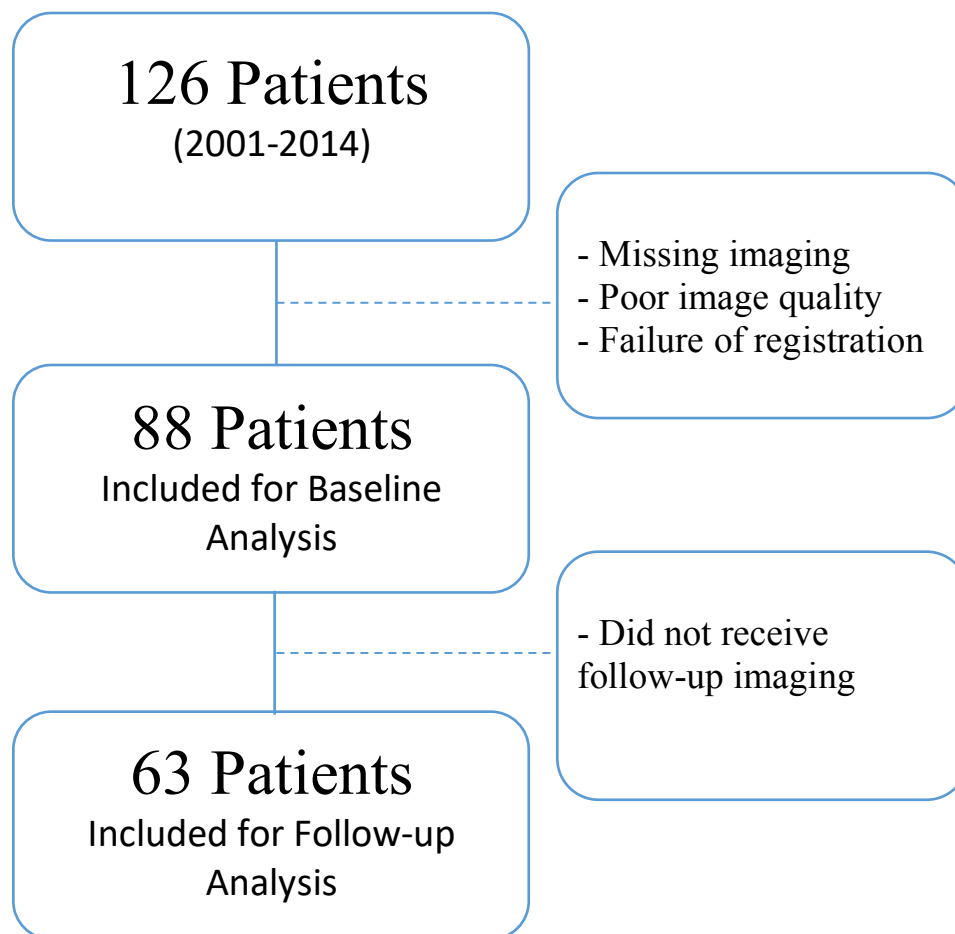


Fig. 1 Flowchart for patient selection process and exclusion criteria

Evaluation and staging

All included patients underwent a full clinical examination and baseline laboratory tests (liver function; serum albumin, prothrombin time, total bilirubin, aspartate transaminase, alanine transaminase). Eastern Cooperative Oncology Group (ECOG) performance status was recorded in all patients.

Intra-arterial therapy

Experienced interventional radiologists performed all procedures. A consistent approach according to our standard institutional protocol was used. Initially, all patients

underwent a diagnostic angiogram to define the hepatic arterial anatomy and to determine portal venous patency. Patients undergoing cTACE were treated with selective (lobar or segmental) injections. A solution containing 100 mg of cisplatin, 50 mg of doxorubicin and 10 mg of mitomycin C in a 1:1 mixture with Lipiodol (Guerbet, France) was infused and followed by administration of 100- to 300- μ m-diameter microspheres (Embospheres, Merit Medical, USA). Substantial arterial flow reduction to the tumor was defined as the technical end point of the procedure. Patients undergoing DEB-TACE received chemoembolization using LC Bead-M1 (70-150 μ m), loaded with 100mg irinotecan (BTG, UK). The beads were mixed with a non-ionic contrast media in the vial immediately prior to use according to the instructions and delivered into the artery slowly (in 1 ml aliquots followed by saline over an approximately 3-5 min period). Patients treated with TARE were subjected to angiographic evaluation and, if required, embolization of collateral arteries was performed to avoid off-target radiation injury. In order to evaluate the degree of hepato-pulmonary shunting and to detect gastrointestinal deposition, 5–6 mCi of ^{99m}Tc -labelled macroaggregated albumin was injected into the hepatic artery. This shunt study preceded the treatment by at least 1 week. Depending on the extent of the disease within the liver, patients received either unilobar or bilobar (right and left) treatment in multiple sessions. In order to avoid liver injury, no whole liver single session infusion was performed. The administration of Y90 microspheres (TheraSpheres®, MDS Nordion, Ottawa, Canada) was performed in accordance with institutional radiation safety guidelines. All patients who received cTACE or DEB-TACE were admitted overnight. Patient who received TARE were discharged the same day of the procedure after clinical monitoring in the recovery area.

MR imaging technique

All patients included in this study underwent a standardized MRI protocol before treatment. MRI was performed on a 1.5-Tesla scanner (Siemens Magnetom Avanto, Erlangen, Germany) using a phased array torso coil. The protocol included breath-hold unenhanced and contrast-enhanced (0.1 mmol/kg intravenous gadopentetate; Magnevist; Bayer, Wayne, NJ) T1-weighted three-dimensional fat-suppressed spoiled gradient-echo imaging (repetition time ms/echo time ms, 5.77/2.77; field of view, 320–400 mm; matrix, 192×160; slice thickness, 2.5 mm; receiver bandwidth, 64 kHz; flip angle, 10°) in the hepatic arterial phase (20 s), portal venous phase (70 s) and delayed phase (3 min).

Image Analysis

Two radiology residents with 2-3 years of experience performed tumor radiological measurements. All measurements made by the two readers were done using standardized electronic calipers using Digital Imaging in Communications and Medicine (DICOM) files. Prior to the measurements, images were examined in axial, coronal and sagittal reconstructions to visually identify the largest tumor dimension (for diameter and enhancement, respectively). The respective slice with the largest dimension of the tumor was then used for individual manual measurements. Native T1 images as well as triphasic contrast-enhanced T1 images were used to visually distinguish tumor enhancement from false-positive hyperintense T1 signal (e.g. from hemorrhage) and measurements were performed on the portal venous phase images (33). The portal venous phase was selected because it is the phase in which hypo-vascular liver metastases such as from lung, breast,

stomach, and colorectal cancer are most conspicuous . The three largest lesions were selected for analysis. The sums for overall tumor diameter and enhancing tumor diameter of the three largest lesions were determined.

3D quantitative image analysis was performed by research medical student MG who had 1 year of experience with the software prototype used in the study (Medisys, Philips Research, Suresnes, France) (27) and was verified by a radiology resident with 2 years of experience. The accuracy and reader-independent reproducibility of the semiautomatic tumor segmentation as well as the radiological–pathological correlation of the technique was described and verified in previous papers (34–37). First, portal venous phase images were registered to the pre-contrast image using an affine transformation method in the BioImage Suite software (Fig. 2a) (38). Then, whole-livers were segmented in three-dimensions using the semi-automatic segmentation software (Fig. 2b). The total liver volume (TLV) was calculated on the basis of this segmentation. The software performed semi-automatic 3D tumor segmentation on the portal venous phase, contrast-enhanced MRI (Fig. 2c). The total tumor volume (TTV) was directly calculated on the basis of this segmentation. Enhancing volumes were determined using the qEASL calculation based on image subtraction (Fig. 2d) (27,39). In brief, the 3D segmentation mask was transferred onto the subtraction image and a region of interest (ROI) was placed into extratumoral liver parenchyma as a reference to calculate the relative enhancement values within the tumor. The patient-specific, average signal intensity within the ROI was then defined as a threshold to estimate enhancement within the 3D mask. Subsequently, enhancing regions were expressed as a percentage of the previously calculated overall tumor volume and visualized using a color map overlay on the portal

venous phase MRI scan. qEASL analysis of both the whole-liver and tumor segmentation mask gives enhancing liver volume (ELV) and enhancing tumor volume (ETV), respectively. ELV divided by TLV gives enhancing liver burden (ELB). ETV divided by TLV gives enhancing tumor burden (ETB). Tumor response after IAT was determined by calculating the change between baseline and one month follow-up imaging in the measured parameters of the same lesions (lesion diameter for RECIST, enhancing lesion diameter for mRECIST, enhancing liver volume for Δ ELV, total tumor volume for vRECIST and enhancing tumor volume for qEASL. Table 1 gives a glossary of terms used in this study and Fig. 3 gives an overview of all anatomic and enhancement-based methods.

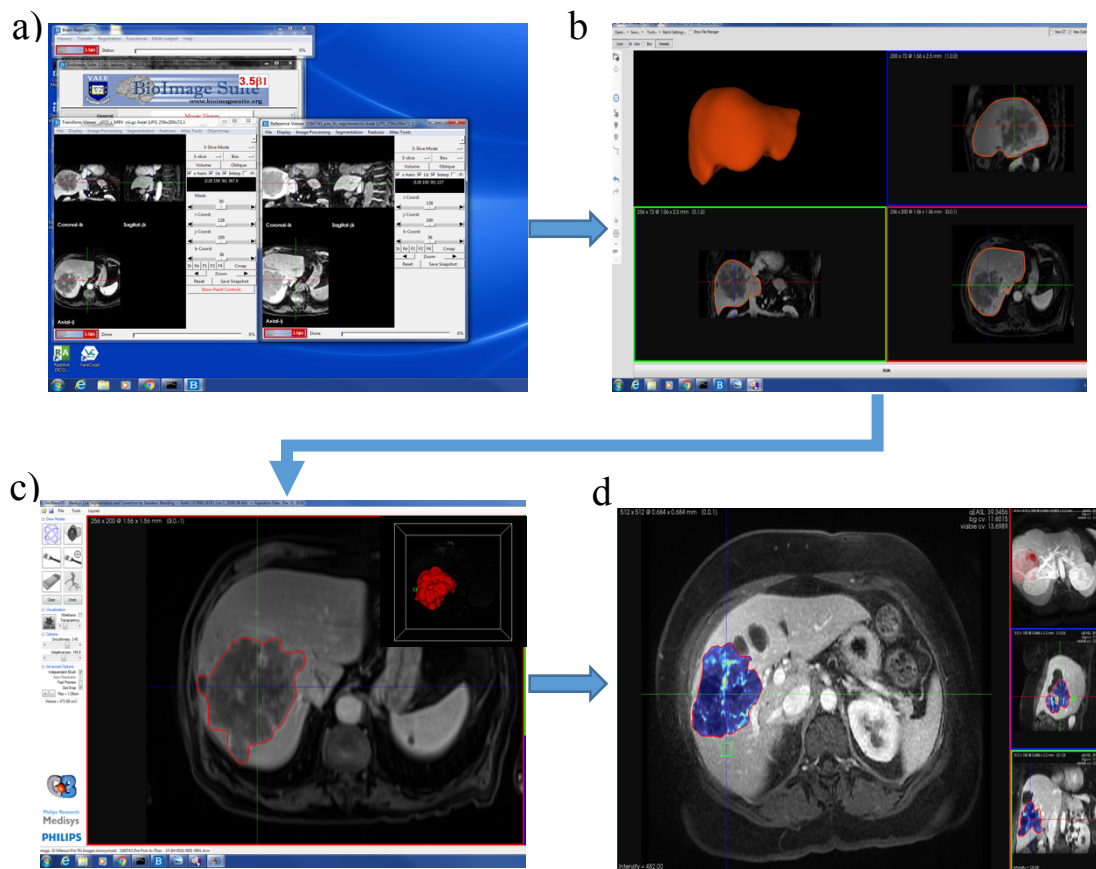


Fig. 2 Image processing workflow. a) Portal venous phase images were registered to the pre-contrast image using an affine transformation method in the BioImage Suite software. b) Whole-livers were segmented in three-dimensions using semi-automatic segmentation software. c) Another software performed semi-automatic 3D tumor segmentation. d) The 3D segmentation mask was transferred onto the subtraction image and a region of interest (ROI) was placed into extratumoral liver parenchyma as a reference to calculate the relative enhancement values within the tumor.

Table 1 Glossary of terms

Term	Abbreviation	Definition
Total Tumor Volume	TTV	Volume of tumor based on tumor segmentation mask
Total Tumor Burden	TTB	TTV divided by liver volume
Enhancing Liver Volume	ELV	Volume of enhancement on whole-liver segmentation mask
Enhancing Liver Burden	ELB	ELV divided by liver volume
Enhancing Tumor Volume	ETV	Volume of enhancement on tumor segmentation mask
Enhancing Tumor Burden	ETB	ETV divided by liver volume
Change in Enhancing Liver Volume	Δ ELV	Percentage change in ELV between baseline and follow-up image
Response Evaluation Criteria In Solid Tumors	RECIST	Percentage change in tumor diameters
Modified RECIST	mRECIST	Percentage change in enhancing tumor diameters
Volumetric RECIST	vRECIST	Percentage change in TTB between baseline and follow-up image
Quantitative EASL	qEASL	Percentage change in ETV between baseline and follow-up image

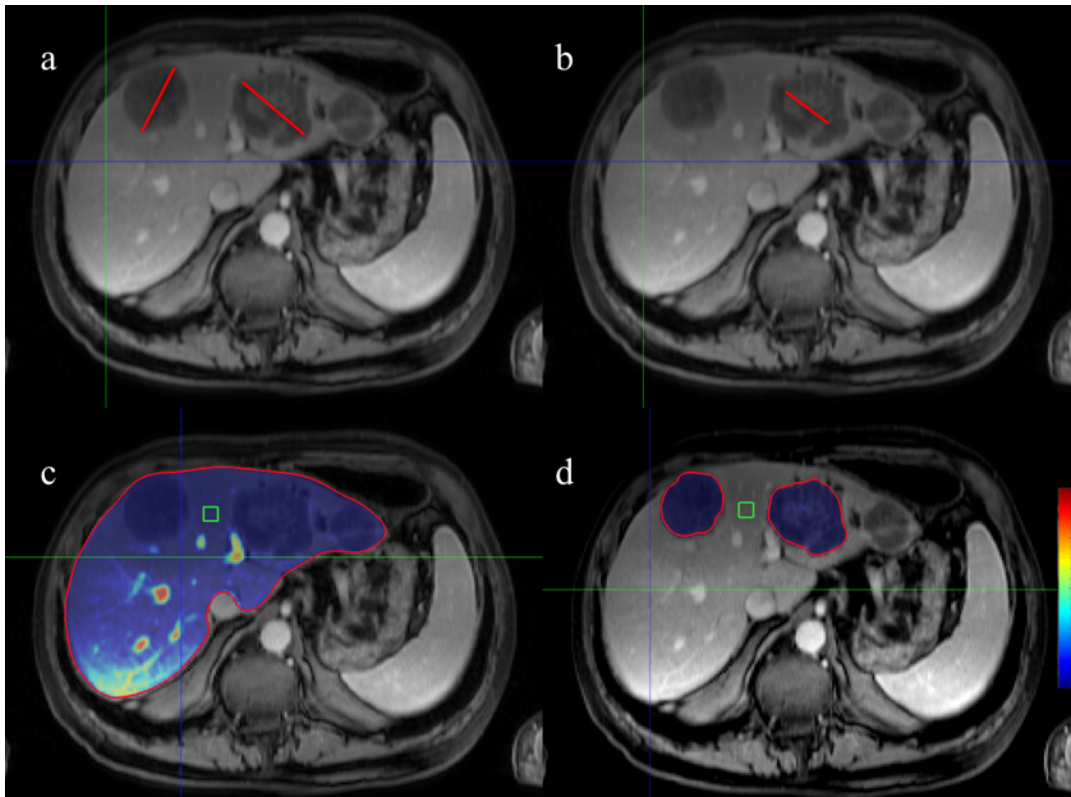


Fig. 3 MRI assessment techniques. **a)** Measurements of one-dimensional overall diameter. **b)** One-dimensional measurement of enhancing tumor diameter. **c)** Red outline shows liver segmentation that gives total liver volume (TLV). Subsequent qEASL analysis gives enhancing liver volume (ELV). ELV/TLV gives enhancing liver burden (ELB). **d)** Red outline shows tumor segmentation which gives total tumor volume (TTV). Subsequent qEASL analysis gives enhancing tumor volume (ETV). ETV/TLV gives enhancing tumor burden (ETB).

Statistical analysis

All statistical computations were performed using the commercial statistical software SPSS (IBM, version 23.0, Armonk, NY, USA). The summary of data was performed using descriptive statistics. Count and frequency were used for categorical variables. Mean and range were used for continuous variables. A non-Gaussian distribution was confirmed and a non-parametric Wilcoxon matched-pair test was used. OS was defined from the date of the IAT session until death or last available follow-up.

In order to stratify patients into two groups based on baseline imaging parameters and 3D response assessment methods, the modified Kaplan-Meier method proposed by Contal and O'Quigley was used to determine optimal thresholds (40). In brief, this method tests each unique value that exists for the given variable as a potential cut-off point. For each potential cut-off point, a Kaplan-Meier analysis and a log-rank test statistic is performed. The lowest p-value and greatest log-rank test statistic is selected as the cut-off point.

Survival curves were estimated with the Kaplan–Meier method and plotted for each stratifying parameter. The median OS and the 95 % confidence interval (CI) for low tumor burden and high tumor burden were calculated for every method. The predictive value of each radiological technique was assessed using Cox proportional hazard ratios (HR). This was followed by a univariate and multivariate analysis, which was performed in two steps. In the first step, a univariate Cox regression model was used to evaluate the association of overall survival with clinical factors assessed on baseline: age, race, sex, number of lesions, treatment type, bilirubin level, existence of extrahepatic metastases, synchronous disease, previous surgery of primary tumor, and previous hepatic resection. In the second step, adjusted hazard ratios for all radiological measurements were estimated from the Cox regression model which simultaneously included the respective radiological method as well as clinical factors that were found to be significantly predictive of overall patient survival ($p < 0.05$) (41).

Results Part I: Baseline MR Imaging Analysis

Patient characteristics and clinical outcome

Baseline patient characteristics are summarized in Table 2. The average age of the cohort at the time of treatment was 59.3 ± 11.4 years. Table 3 gives disease characteristics and treatment history. A majority of patients ($N=68$, 77.3%) had multifocal disease. The majority of patients (96.6%) received previous colorectal resection, but only one patient received previous hepatic resection. The cohort is approximately evenly split between those who received TARE ($N=47$, 53.4%) and those who received TACE ($N=41$, 46.6%). All IATs were technically successful and no major toxicities were reported. The mean interval between baseline imaging and IAT was 19.8 days (range, 1-60 days). Median OS of the cohort was 7.6 months (95% CI 6.1-9.0), and by the end of the study observation date (December 1st, 2016), a total of 79 patients (89.8%) were deceased.

Table 2 Baseline Patient and Tumor Characteristics

Parameter	N (%)
<u>Demographics</u>	
Age	
<65	61 (69)
≥65 years	27 (31)
Sex	
Male	60 (68)
Female	28 (32)
Race	
White	68 (77)
African-American	14 (16)
Other	6 (7)
ECOG Score	
0	59 (67)
1	26 (30)
2	3 (3)
Bilirubin (mg/dL)	
≤1.2	77 (88)
>1.2	11 (12)

Table 3 Disease Characteristics and Treatment History

Parameter	N (%)
Number of lesions/patient	
1	20 (23)
2	13 (15)
3	8 (9)
≥4	47 (53)
First IAT Received	
TARE	47 (53)
TACE	41 (47)
Synchronous disease	
Yes	52 (59)
No	36 (41)
Extrahepatic metastases	
Yes	31 (35)
No	57 (65)
Tumor location	
Bilobar	68 (77)
Unilobar	20 (23)
Previous Systemic Chemotherapy	
Yes	77 (88)
No	11 (13)
Previous Surgery of Primary Tumor	
Yes	85 (97)
No	3 (3)
Previous Hepatic Resection	
Yes	1 (1)
No	87 (99)

Image Analysis

Liver and tumor characteristics as well as the results of 1D and 3D measurements are summarized in Table 4. One-dimensional analysis gave a mean overall tumor diameter of 15.6 ± 6.8 cm and an enhancing tumor diameter of 8.9 ± 4.1 cm. As for 3D analysis, mean liver volume was 2165 ± 778 cm³ (range 862-4583 cm³). Whole-liver 3D assessment gave an ELV of 818 ± 433 cm³ (range 104-2262 cm³) and an ELB of $38.1 \pm 16.4\%$ (range 10.1-79.3%). Three-dimensional measurements acquired from the tumor segmentations gave an ETV of 94.7 ± 163 cm³ (range 0.01- 886 cm³) and an ETB of $3.6 \pm 19.4\%$ (range 0.01-24.3%). Table 5 gives the threshold value used to stratify the cohort into high and low burden groups for each parameter based on the modified Kaplan-Meier method as already described.

Table 4 Tumor/Liver Characteristics and 1D and 3D measurements

Parameter	
Liver Volume (cm ³)	
Mean	2165
Range	862-4583
<u>1D Measurements</u>	
Overall Tumor Diameter (cm)	
Mean	15.6
SD	6.8
Enhancing Tumor Diameter (cm)	
Mean	8.9
SD	4.1
<u>3D Measurements</u>	
Enhancing Liver Volume [ELV] (cm³)	
Mean	818
SD	433
Enhancing Liver Burden [ELB] (%)	
Mean	38.1
SD	16.4
Total Tumor Volume [TTV] (cm³)	
Mean	499
SD	626
Total Tumor Burden [TTB] (%)	
Mean	19
Range	0.2-99
Enhancing Tumor Volume [ETV] (cm³)	
Mean	94.7
SD	163
Enhancing Tumor Burden [ETB] (%)	
Mean	3.6
Range	0.01-24.3

Table 5 Optimal cutoff values for high and low tumor burden

Image Parameter	Cutoff
Overall tumor diameter	11.5 cm
Enhancing tumor diameter	8.0 cm
Total tumor volume (TTV)	335 cm ³
Total tumor burden (TTB)	15%
Enhancing liver volume (ELV)	1060 cm ³
Enhancing liver burden (ELB)	32%
Enhancing tumor volume (ETV)	60 cm ³
Enhancing tumor burden (ETB)	3.2%

Survival Analysis

Univariate analysis of baseline clinical parameters identified a significant correlation between the lobar distribution of disease (bilobar disease, hazard ratio [HR] 2.12 [95 % CI 1.22-3.7], $p=0.01$), ECOG score (ECOG >0, HR 1.79 [95% CI 1.09-2.9], $p=0.02$), bilirubin level (bilirubin >1.2 mg/dL, HR 1.9 [95% CI 1.1-3.6], $p=0.05$), and previous systemic chemotherapy (HR 0.48 [95 % CI 0.24-0.97], $p=0.04$) with OS. The other baseline characteristics included for univariate analysis (age, race, sex, number of lesions, treatment type, existence of extrahepatic metastases, synchronous disease, previous surgery of primary tumor, and previous hepatic resection) did not show significant correlation with OS.

For the diameter-based thresholds, the log-rank test demonstrated that survival curves showed good separation when stratified both by overall tumor diameter ($p=0.004$)

and enhancing tumor diameter ($p<0.001$). 68% of patients were classified into the high tumor burden group for overall tumor diameter, and these patients had a median OS of 6.0 months (95% CI 3.9-8.0). 56% of patients were classified into the high tumor burden group for enhancing tumor diameter, and had a median OS of 5.8 months (95% 4.8-6.9).

In terms of volume-based thresholds, both TTV ($p=0.003$) and TTB ($p=0.004$) demonstrated good separation of survival curves based on the log-rank test. A minority of patients were classified into the high tumor burden group based on TTV (40%) and had a median OS of 5.8 months (95% CI 3.3-8.4), while about half of patients were based on TTB (45%) and had also had a median OS of 5.8 months (95% CI 3.2-8.4).

As for 3D enhancement based-criteria, ELV ($p=0.03$), ETV ($p<0.001$) and ETB ($p=0.001$) all demonstrated good separation of Kaplan-Meier curves, but ELB did not ($p=0.09$) (Fig. 4). A minority of patients were classified into the high tumor burden group based on ELV (26%), and this group had a median OS of 4.6 months (95% CI 1.6-7.7). 33% of patients were in the high tumor burden group based on ETV, and had a median OS of 4.4 months (95% CI 2.9-5.8). Finally, only 30% of patients were classified into the high burden group based on ETB, and this group had a median OS of 4.6 months (95% CI 2.2-7.1).

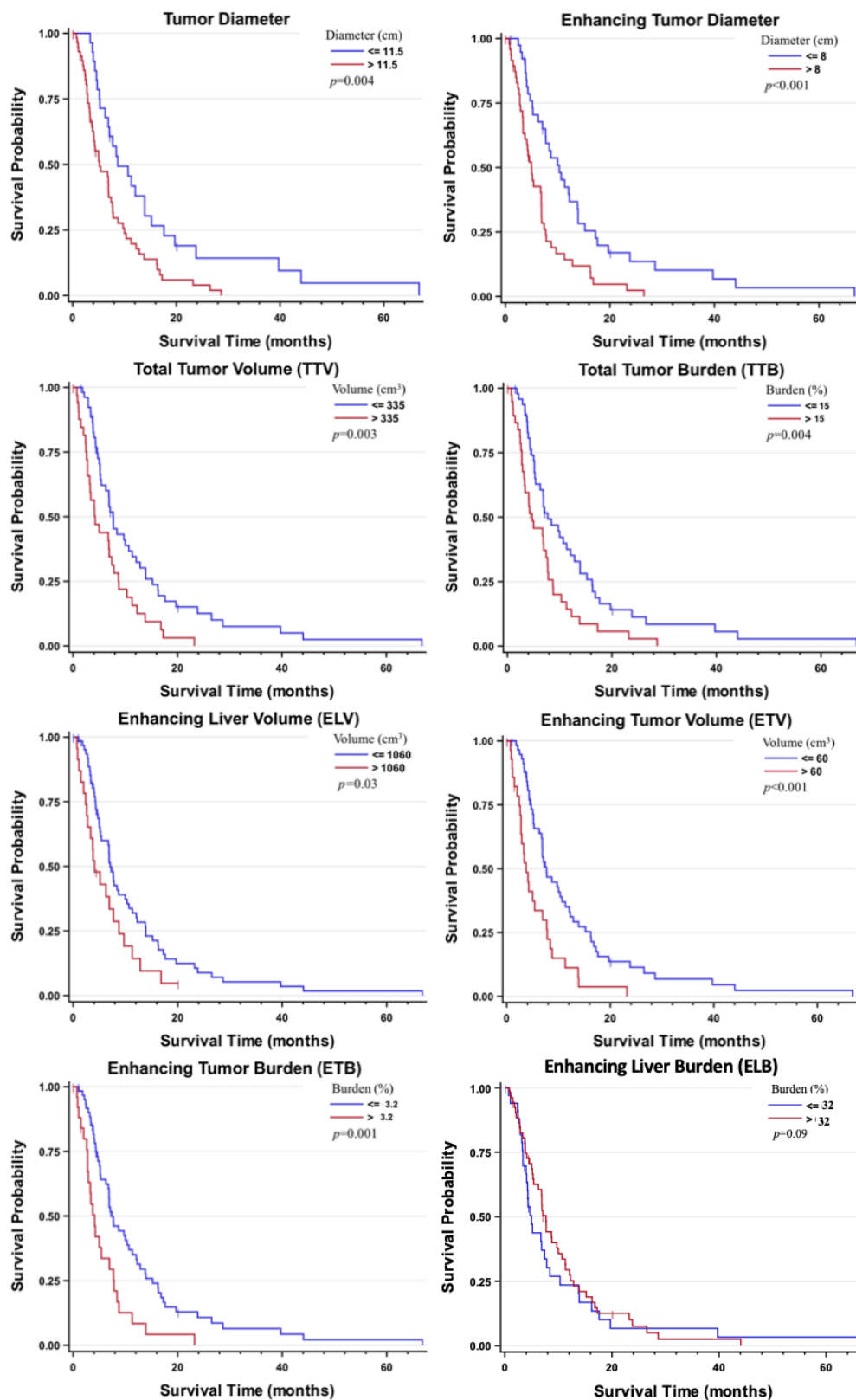


Fig. 4 Kaplan-Meier survival curves plotted for each image assessment technique. ELB was the only parameter that did not demonstrate significant separation of curves.

Multivariate Analysis

When adjusting for bilobar disease, ECOG score, bilirubin level and previous systemic chemotherapy, significant correlation with OS was no longer seen with overall diameter, TTB, or ELV. As shown in Table 6, patients in the high tumor burden group for enhancing tumor diameter had a hazard ratio of 2.1 (95% CI 1.3-3.4, $p=0.004$). Patients stratified into the high tumor burden group based on TTV had a HR of 1.7 (95% CI 1.1-2.8, $p=0.04$). The greatest hazard ratios were achieved when patients were stratified on the basis on ETV (HR 2.3, 95% CI 1.4-3.9, $p<0.001$) and ETB (HR 2.4, 95% CI 1.4-4.0, $p=0.001$).

Table 6 Statistical analysis of median overall survival

Method	N (%)	Survival analysis Median (95 % CI)	Univariate analysis		Multivariate analysis	
			HR (95 % CI)	<i>P</i> value	HR (95 % CI)	<i>P</i> value
Overall Diameter						
≤11.5 cm	28 (32)	9.1 (4.9-13.3)	2.1 (1.3-3.4)	0.004	1.34 (0.8-2.3)	0.3
>11.5 cm	60 (68)	6.0 (3.9-8.0)				
Enhancing Diameter						
≤8 cm	39 (44)	11.1 (7.5-14.7)	2.3 (1.4-3.7)	<0.001	2.1 (1.3-3.4)	0.004
>8 cm	49 (56)	5.8 (4.8-6.9)				
TTV						
≤335 cm ³	53 (60)	8.9 (7.2-10.5)	2.0 (1.3-3.2)	0.003	1.7 (1.1-2.8)	0.04
>335 cm ³	35 (40)	5.8 (3.3-8.4)				
TTB						
≤15%	48 (55)	8.9 (5.4-12.3)	1.9 (1.2-3.0)	0.006	1.4 (0.8-2.5)	0.2
>15%	40 (45)	5.8 (3.2-8.4)				
ELV						
≤1060 cm ³	65 (74)	8.0 (6.5-9.5)	1.7 (1.0-2.9)	0.03	1.6 (0.9-2.7)	0.08
>1060 cm ³	23 (26)	4.6 (1.6-7.7)				
ELB						
≤32%	34 (39)	5.6 (5.0-6.2)	0.7 (0.4-1.1)	0.09		
>32%	54 (61)	9.0 (7.1-10.9)				
ETV						
≤60	59 (67)	9.0 (7.0-11.0)	2.4 (1.5-3.9)	<0.001	2.3 (1.4-3.9)	<0.001
>60	29 (33)	4.4 (2.9-5.8)				
ETB						
≤3.2%	62 (70)	8.6 (6.5-10.6)	2.3 (1.4-3.8)	0.001	2.4 (1.4-4.0)	0.001
>3.2%	26 (30)	4.6 (2.2-7.1)				

Results Part II: Treatment Response Assessment

Patient characteristics and clinical outcome

Patient characteristics for this smaller follow-up cohort are again summarized in Table 7 and Table 8. No statistically significant differences exist in demographic and treatment history characteristics between the baseline analysis cohort and follow-up analysis cohort. The average age of the cohort at the time of treatment was 59.6 ± 11.4 years. The mean interval between baseline imaging and IAT was 19.6 days (range, 1-50 days). The mean interval between IAT and follow-up imaging was 34.3 days (range, 22-51 days). Median OS of the cohort was 9.0 months (95% CI 7.5-10.6), and by the end of the study observation date (December 1st, 2016), a total of 57 (90.5%) were deceased. The OS is greater than that of the baseline analysis cohort. This could be partly explained by the fact that patients who died before they could receive follow-up imaging were not included in this cohort. However, the difference is not significant ($p=0.584$).

Table 7 Follow-up Cohort Patient and Tumor Characteristics

Parameter	N (%)
<u>Demographics</u>	
Age	
<65	42 (67)
≥65 years	21 (33)
Sex	
Male	45 (71)
Female	18 (29)
Race	
White	49 (78)
African-American	10 (16)
Other	4 (6)
ECOG Score	
0	40 (64)
1	19 (30)
2	3 (5)
Bilirubin (mg/dL)	
≤1.2	57 (90)
>1.2	6 (10)

Table 8 Follow-up Cohort Disease Characteristics and Treatment History

Parameter	N (%)
Number of lesions/patient	
1	15 (24)
2	12 (19)
3	4 (6)
≥4	32 (51)
First IAT Received	
TARE	33 (52)
TACE	30 (48)
Synchronous disease	
Yes	37 (59)
No	26 (41)
Extrahepatic metastases	
Yes	20 (32)
No	43 (68)
Tumor location	
Bilobar	48 (76)
Unilobar	15 (24)
Previous Systemic Chemotherapy	
Yes	57 (90)
No	6 (10)
Previous Surgery of Primary Tumor	
Yes	62 (98)
No	1 (2)
Previous Hepatic Resection	
Yes	1 (2)
No	62 (98)

Survival Analysis

Univariate analysis of baseline clinical parameters again identified a significant correlation between OS and lobar distribution of disease (bilobar disease, hazard ratio [HR] 2.45 [95 % CI 1.25-4.781, $p=0.01$) and ECOG score (ECOG >0 , HR 1.87 [95% CI 1.06-3.28], $p=0.03$). However, previous systemic chemotherapy (HR 0.54 [95 % CI 0.21-1.39], $p=0.20$) and bilirubin level (HR 1.0 [95 % CI 0.4-2.4], $p=0.90$) did not have a significant correlation in the follow-up cohort with OS. The other baseline characteristics included for univariate analysis (age, race, sex, number of lesions, treatment type, existence of extrahepatic metastases, synchronous disease, previous surgery of primary tumor, and previous hepatic resection) also again did not show significant correlation with OS.

Single MR Image Analysis: Baseline and Follow-up Images

To perform direct head-to-head comparisons of the strength of the various measurement techniques as both staging biomarkers as well as surrogates for treatment response, imaging analysis for this smaller cohort was repeated for the baseline images and also performed on the follow-up images. Whole-liver analysis was not repeated as Part I did not demonstrate success using these criteria. Table 9 summarizes survival analysis and univariate and multivariate Cox proportional hazard model analysis for the baseline images of this cohort while Table 10 summarizes these findings for the follow-up images.

Table 9 Statistical analysis of median overall survival based on baseline imaging analysis

Method	N (%)	Survival analysis Median (95 % CI)	Univariate analysis		Multivariate analysis	
			HR (95 % CI)	<i>P</i> value	HR (95 % CI)	<i>P</i> value
Overall Diameter						
≤11.5 cm	23 (36)	9.1 (4.1-14.1)	1.4 (0.816-2.4)	0.2		
>11.5 cm	40 (63)	8.1 (5.9-10.4)				
Enhancing Diameter						
≤8 cm	34 (54)	10.8 (6.7-15.0)	1.7 (1.0-2.9)	0.06		
>8 cm	29 (46)	7.4 (5.4-9.4)				
TTV						
≤335 cm ³	41 (65)	9.1 (6.6-11.6)	1.3 (0.98-1.7)	0.08	1.42 (1.1-2.9)	0.24
>335 cm ³	22 (35)	7.6 (4.3-10.3)				
TTB						
≤15%	37 (59)	10.6 (6.0-15.2)	1.6 (0.9-2.7)	0.08		
>15%	26 (41)	7.6 (4.0-11.2)				
ETV						
≤60	45 (71)	10.6 (8.1-13.1)	2.1 (1.2-3.7)	0.02	1.9 (1.1-3.6)	0.03
>60	19 (29)	7.6 (4.2-10.9)				
ETB						
≤3.2%	46 (73)	10.6 (8.0-13.2)	2.1 (1.1-3.7)	0.02	2.2 (1.2-4.1)	0.01
>3.2%	17 (27)	7.6 (4.4-10.7)				

Table 10 Statistical analysis of median overall survival based on follow-up imaging analysis

Method	N (%)	Survival analysis Median (95 % CI)	Univariate analysis		Multivariate analysis	
			HR (95 % CI)	<i>P</i> value	HR (95 % CI)	<i>P</i> value
Overall Diameter						
≤11.5 cm	20 (32)	9.1 (4.7-13.5)	1.3 (0.7-2.2)	0.4		
>11.5 cm	43 (68)	8.1 (6.2-10.1)				
Enhancing Diameter						
≤8 cm	45 (71)	9.1 (7.0-11.2)	1.6 (0.9-2.9)	0.1		
>8 cm	18 (29)	7.4 (4.8-10.0)				
TTV						
≤335 cm ³	37 (59)	10.6 (6.2-15.0)	2.0 (1.2-3.4)	0.01	1.7 (0.98-3.0)	0.06
>335 cm ³	26 (41)	6.9 (4.5-9.3)				
TTB						
≤15%	36 (57)	11.1 (6.8-15.4)	1.8 (1.1-3.0)	0.03	1.4 (0.8-2.5)	0.2
>15%	27 (43)	6.4 (3.9-8.9)				
ETV						
≤60	47 (75)	10.8 (6.9-14.7)	2.9 (1.6-5.4)	0.01	12.4 (1.2-4.5)	< 0.01
>60	16 (25)	5.9 (2.7-9.2)				
ETB						
≤3.2%	37 (59)	12.2 (9.6-14.9)	1.9 (1.1-3.2)	0.02	1.4 (0.8-2.5)	0.2
>3.2%	26 (41)	6.9 (4.5-9.2)				

ID Measurements

For this smaller cohort, diameter-based measurements on baseline imaging were not successful at stratifying patients by survival. 63% of patients were classified into the high tumor burden group for overall tumor diameter, and these patients had a median OS of 8.1 months (95% CI 5.9-10.4), which was not statistically significant from the low tumor burden group. 46% of patients were classified into the high tumor burden group for enhancing tumor diameter, and had a median OS of 7.4 months (95% CI 5.4-9.4). The log-rank test demonstrated a marginal statistically significant difference in the survival

curves ($p=0.05$, survival curves not shown). Hazard ratio modeling did not demonstrate significance in multivariate analysis. Diameter-based measurements on follow-up images demonstrated similar results with neither overall diameter nor enhancing diameter able to stratify patients by survival with statistical significance.

For the diameter-based thresholds, the log-rank test demonstrated that survival curves showed good separation when stratified both by overall tumor diameter ($p=0.004$) and enhancing tumor diameter ($p<0.001$). 68% of patients were classified into the high tumor burden group for overall tumor diameter, and these patients had a median OS of 5.2 months (95% CI 3.8-7.4). 56% of patients were classified into the high tumor burden group for enhancing tumor diameter, and had a median OS of 5.0 (95% 3.4-6.9).

3D Measurements

For volume-based measurements, neither TTV ($p=.07$) nor TTB ($p=.08$) demonstrated statistically significant separation of survival curves based on the log-rank test on baseline images. However, both criteria resulted in good separation of survival curves on follow-up images ($p=.01$ and $p=.03$, respectively), although these differences were not significant when controlling for other risk factors (ECOG score and unilobar vs. bilobar).

In terms of 3D, enhancement-based criteria, both ETV and ETB again consistently resulted in good separation of survival curves for both baseline and follow-up images. These differences remained when controlling for other risk factors for all criteria except ETB in follow-up images (HR 1.4 [95% CI 0.8-2.5], $p=0.2$).

Response Assessment

The mean changes between baseline and 1 month follow-up images based on various 1D and 3D measurement criteria are given in Table 11 as well as the thresholds used to separate patients into responders (R) and non-responders (NR). For, RECIST and mRECIST, patients were classified as R if the overall diameter or enhancing diameter, respectively, decreased by 30% or more, as per RECIST and mRECIST guidelines (42). Enhancing liver volume increased on average by 13.8% (range -83.2-262%). Patients were categorized as R if the percent change in ELV (Δ ELV) was negative and classified as non-responders if Δ ELV was positive. Change in ELB was not included in response assessment as it is related to Δ ELV ($ELB = ELV/TTV$). Total tumor volume on average increased by 31.8% (range -50.6-551%). Patients were classified as R if the volume decreased or did not increase by more than 50%. Finally, enhancing tumor volume increased on average by 69.4%. Patients were classified as R if enhancing tumor volume decreased by more than 65% (range -99.5%-2219%).

Table 11 Response assessment measurements

Parameter	
Liver Volume (cm ³)	
Mean	2210
Range	848-5034
<u>1D Measurements</u>	
RECIST (%)	
Mean	0.04
Range	-33.4-64.5
Threshold	-30
mRECIST (%)	
Mean	-11.1
Range	-100-73.0
Threshold	-30
<u>3D Measurements</u>	
Enhancing Liver Volume	
Change [Δ ELV] (%)	
Mean	13.8
Range	-83.2-262
Threshold	0
Change in total tumor volume	
(vRECIST) (%)	
Mean	31.8
Range	-50.6-551
Threshold	50
Change in Enhancing Tumor	
Volume (qEASL) (%)	
Mean	69.35
Range	-99.5-2219
Threshold	-65

1D Measurements

Table 12 gives a summary of overall survival using univariate and multivariate analysis. When using RECIST measurements, only 1 patient was classified as a responder. Therefore, OS analysis was not performed based on RECIST criteria. Using mRECIST criteria, 20 patients (32%) were classified as R and had an OS of 9.8 months

(95% CI 5.9-13.7) and 43 patients (68%) were classified as NR with an OS of 7.4 months (95% CI 4.7-10.1). Stratifying Kaplan-Meier curves based on mRECIST criteria did not achieve statistical significance ($p=0.1$) (Fig. 5a).

Table 12 Statistical analysis of median OS based on response assessment measurements

Method	R/NR	N (%)	Survival analysis	Univariate analysis		Multivariate analysis	
			Median (95 % CI)	HR (95 % CI)	<i>P</i> value	HR (95 % CI)	<i>P</i> value
RECIST							
≥30% decrease	R	1 (2)	-				
<30% decrease	NR	62 (98)	9.1 (7.4-10.7)				
mRECIST							
≥30% decrease	R	20 (32)	9.8 (5.9-13.7)	1.5 (0.9-2.7)	0.1		
<30% decrease	NR	43 (68)	7.4 (4.7-10.1)				
ΔELV							
<0%	R	31 (49)	11.8 (9.4-14.2)	1.3 (0.8-2.3)	0.3		
≥0%	NR	32 (51)	6.6 (4.3-8.8)				
vRECIST							
<50% increase	R	48 (76)	9.8 (7.5-12.0)	2.1 (1.1-4.0)	0.02	2.1 (1.1-4.0)	0.03
Greater than ≥50% increase	NR	15 (24)	6.4 (5.2-7.6)				
qEASL							
≥56% decrease	R	19 (30)	14.3 (10.0-18.6)	1.7 (0.9-3.0)	0.08		
<56% decrease	NR	44 (70)	8.0 (5.6-10.4)				

3D Measurements

When quantifying tumor response with ΔELV, 31 patients (49%) were classified as R and 32 patients (51%) were classified as NR. Stratifying Kaplan-Meier curves using this stratification method did not demonstrate good separation of survival curves (Fig. 5b, $p=0.3$). When using the vRECIST technique, 48 patients (76%) were R and had a median

OS of 9.8 months (95% CI 7.5-12.0) while 15 patients (24%) were NR and had a median OS of 6.4 months (95% CI 5.2-7.6). The log-rank test demonstrated good separation of survival curves ($p=0.02$, Fig. 5c). Univariate Cox regression also demonstrated poorer survival in the NR group (HR 2.1 95% CI 1.1-4.0, $p=0.02$). This was unchanged when controlling for other risk factors in multivariate analysis. When using the qEASL method, 19 patients (30%) were classified as R and had a median OS of 14.3 months (95% CI 10.0-18.6), while 44 patients (70%) were classified as NR and had a median OS of 8.0 (95% CI 5.6-10.4). However, separation of survival curves was not significant by this method ($p=0.08$, Fig. 5d).

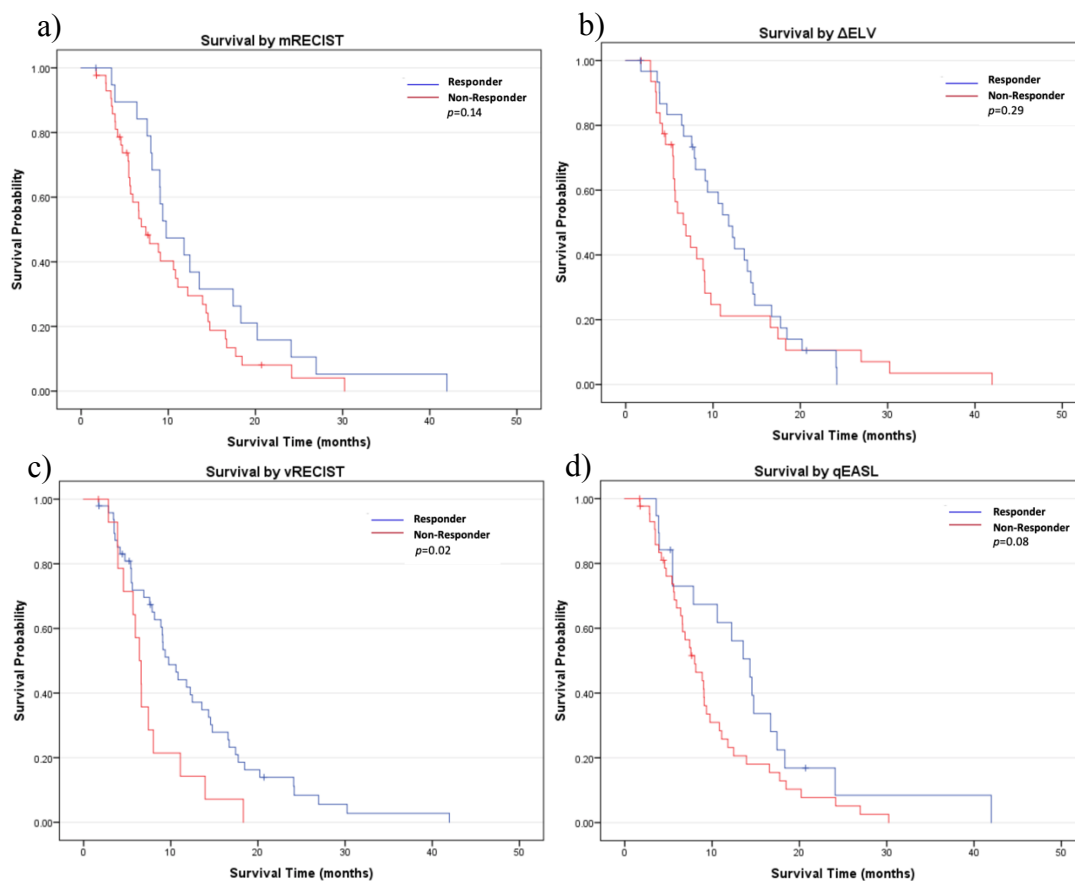


Fig. 5 Kaplan-Meier survival curves plotted for response assessment methods. vRECIST was the only method to demonstrate good separation of survival curves based on the log-rank test.

Discussion

The major finding of this study was that enhancing tumor volume (ETV) was the best candidate tested for a novel prognostic staging imaging biomarker. Enhancing tumor burden (ETB) was also able to predict survival on baseline imaging, but was not significant when used on follow-up imaging and controlling for other risk factors. While enhancing diameter and non-enhancement volumetric methods were also predictors of survival, they were inferior to ETV and ETB. Prior to the current study, it could be hypothesized that since greater enhancement suggests greater tumor vascularity, tumor enhancement should be a good prognostic indicator, as it would allow greater penetration of the tumor by therapeutic agents delivered by IATs. However, the data presented here instead suggests that greater tumor vascularity indicates a more aggressive tumor phenotype, which has a negative effect on patient survival. This idea has also been corroborated in other non-CRC etiologies of liver cancer (28,29,31,32). Intuitively, it could be reasoned that ETB should be superior to ETV, since ETB places the volume of enhancing tumor in relation to the volume of normal tumor parenchyma. However, ETB and ETV demonstrated similar results in this study. A larger sample size may be necessary to help differentiate these two parameters.

Currently, there is no satisfactory staging method for advanced colorectal cancer (18). The current system (AJCC, 8th edition) utilizes the TNM staging system for colorectal cancer, which groups all metastatic disease as stage IV. However, extensive variation in prognosis and treatment patterns exists among this group. The 5-year survival expectancy of metastatic disease that is resectable with curative intent is about 20-45%, while it is less than 5% when not (43). Depending on number, size and location of liver

metastases, treatments can range from surgical resection, ablation, chemotherapy, TACE and radioembolization (43–45). This study demonstrates that volumetric, enhancement-based criteria such as ETV or ETB, combined with clinical data, such as liver function tests, KRAS gene mutation status and performance status, may be the basis of a prognostic staging system for patients with liver dominant colorectal cancer metastases. Such a staging system may be analogous to the Barcelona Clinic Liver Cancer (BCLC) used to guide management of patients with hepatocellular carcinoma (46). A combined imaging and staging system for advanced colorectal cancer may help standardize treatment guidelines and help patients make informed treatment decisions.

In terms of whole-liver analysis, ELV and ELB were not found to be significant predictors of survival in univariate and multivariate analysis. This is contrary to a study of neuroendocrine liver metastases which found that whole liver enhancing tumor burden was a good predictor of survival (29). There are several potential explanations for this. First, colorectal cancer metastases, like most liver metastases, are relatively hypovascular tumors (47). This, in turn, results in relatively less enhancement from the tumor in relation to other sources of enhancement, such as blood vessels, that makes it difficult to truly distinguish high enhancing burden from low enhancing burden. Another source of false-enhancement in this study was the bias field, which is a low-frequency intensity variation that occurs in MR images due to the imperfection of the magnetic field and inhomogeneity of the scanned object (48). While bias field correction algorithms exist, these are not yet sophisticated enough to correct the bias field without also altering tumor-related enhancement. The development of a whole-liver approach to enhancement analysis and staging is attractive because whole-liver segmentation is much less time-

intensive than tumor segmentation. It also removes much of the subjectivity that arises from segmentations between different readers. In order to overcome the current shortcomings with whole-liver analysis, there is a need for automatic segmentation software that can classify tissue into normal parenchyma, tumor, and vessel. The advent of intelligent machine-learning algorithms may be the solution for this technological barrier that needs to be taken in order to make whole-liver enhancement a useful method for staging (49).

In terms of response assessment measurement methods, vRECIST was successfully able to stratify patients by OS, while Δ ELV and qEASL were not. The reasons Δ ELV was not a good marker of treatment response were likely the same as the reasons given above for why ELV was not a good staging marker. The results of this study are in contrast to another study of a smaller cohort of patients with colorectal cancer metastases to the liver treated with IATs which found that qEASL was able to predict survival (28). An explanation for why ETV had good performance as a staging marker, but qEASL was not successful as a response marker in this study may be related to the significant effect the selection of the ROI has on the calculated ETV. Although care was taken to select similar regions of the liver as the ROI in the baseline and follow-up image for each patient, changes in the bias field or overall enhancement characteristics of normal parenchyma resulted in large changes in ETV that may not be related to tumor physiology. Again, a machine learning approach may serve to improve the use of qEASL as a response assessment tool. If normal liver parenchyma can be automatically segmented, then the average signal intensity of the entirety of normal parenchyma can be

used to normalize the relative enhancement within the tumor, rather than only a 10 cm³ region of interest selected by the ROI.

This study has several limitations. This is a single-institution retrospective study that is susceptible to selection bias. Additionally, the thresholds used to stratify the cohort in this study were determined from statistical analysis and may not be broadly applicable. It is worth noting, however, that the threshold used for ETV (60 cm³) and TTV (3.2%) are similar to values used in studies of different cohorts (31,32). Another limitation in this study is that patients who received cTACE or DEB-TACE were grouped and analyzed together since few patients in this cohort received DEB-TACE (~8%). However, DEB-TACE has an important technical difference from cTACE, notably that cTACE is performed until near stasis of flow in the selected tumor-feeding artery is achieved, while stasis is not an endpoint of DEB-TACE when using irinotecan. Future studies should aim to recruit a larger cohort of DEB-TACE patients to determine if a difference in the accuracy of staging or response assessment imaging biomarkers exists. Finally, as this retrospective analysis was performed on prospectively collected data, not all risk factors could be controlled for. For example, the status of KRAS mutation in these patients, which is correlated to poor response to certain anti-epidermal growth factor receptor therapies, is unknown (50).

In summary, our findings support the use of volumetric and enhancement-based biomarkers in baseline MR imaging in patients who will be undergoing TACE or TARE. The association between tumor enhancement and patient survival warrants further investigation for possible inclusion in a new staging system for colorectal cancer metastases to the liver. Additionally, a volumetric approach to treatment response

assessment is superior to the currently established one-dimensional methods. However, enhancement-based, volumetric treatment response methods such as Δ ELV and qEASL need further refining before they can be utilized in patients with colorectal cancer metastases to the liver being treated with IATs. The currently accepted one-dimensional and two-dimensional criteria were developed at a time when computer-assisted imaging analysis was much less sophisticated than it is today. To meet the changing nature of imaging technology and take advantage of the advent of semi- and fully-automated volumetric measurements, an update to staging and response criteria may be warranted.

References

1. Lozano R, Naghavi M, Foreman K, et al. Global and regional mortality from 235 causes of death for 20 age groups in 1990 and 2010: a systematic analysis for the Global Burden of Disease Study 2010. *Lancet* (London, England). 2012;380(9859):2095–2128.
2. DeSantis CE, Lin CC, Mariotto AB, et al. Cancer treatment and survivorship statistics, 2014. *CA Cancer J Clin*. 64(4):252–271.
3. Engstrom PF, Arnoletti JP, Benson AB, et al. NCCN Clinical Practice Guidelines in Oncology: colon cancer. *J Natl Compr Canc Netw*. 2009;7(8):778–831.
4. Bozzetti F, Doci R, Bignami P, Morabito A, Gennari L. Patterns of failure following surgical resection of colorectal cancer liver metastases. Rationale for a multimodal approach. *Ann Surg*. 1987;205(3):264–270.
5. Haddad AJ, Bani Hani M, Pawlik TM, Cunningham SC. Colorectal liver metastases. *Int J Surg Oncol*. 2011;2011:285840.
6. Lam VWT, Spiro C, Laurence JM, et al. A systematic review of clinical response and survival outcomes of downsizing systemic chemotherapy and rescue liver surgery in patients with initially unresectable colorectal liver metastases. *Ann Surg Oncol*. 2012;19(4):1292–1301.
7. Saltz LB, Douillard JY, Pirotta N, et al. Irinotecan plus fluorouracil/leucovorin for metastatic colorectal cancer: a new survival standard. *Oncologist*. 2001;6(1):81–91.
8. Fiorentini G, Aliberti C, Tilli M, et al. Intra-arterial infusion of irinotecan-loaded drug-eluting beads (DEBIRI) versus intravenous therapy (FOLFIRI) for hepatic metastases from colorectal cancer: final results of a phase III study. *Anticancer Res*. 2012;32(4):1387–1395.
9. Van Hazel G, Blackwell A, Anderson J, et al. Randomised phase 2 trial of SIR-Spheres plus fluorouracil/leucovorin chemotherapy versus fluorouracil/leucovorin chemotherapy alone in advanced colorectal cancer. *J Surg Oncol*. 2004;88(2):78–85.
10. Hendlisz A, Van den Eynde M, Peeters M, et al. Phase III trial comparing protracted intravenous fluorouracil infusion alone or with yttrium-90 resin microspheres radioembolization for liver-limited metastatic colorectal cancer refractory to standard chemotherapy. *J Clin Oncol*. 2010;28(23):3687–3694.
11. Benson AB, Venook AP, Al-Hawary MM, et al. NCCN Guidelines Insights: Colon Cancer, Version 2.2018. *J Natl Compr Canc Netw*. 2018;16(4):359–369.
12. Foubert F, Matysiak-Budnik T, Toucheffeu Y. Options for metastatic colorectal cancer beyond the second line of treatment. *Dig Liver Dis*. 2014;46(2):105–112.
13. Pan L-H, Zhao C, Ma Y-L. Is Y90 Radioembolization Superior or Comparable to Transarterial Chemoembolization for Treating Hepatocellular Carcinoma? *Gastroenterology*. 2017;152(6):1627–1628.
14. de Baere T, Arai Y, Lencioni R, et al. Treatment of Liver Tumors with Lipiodol TACE: Technical Recommendations from Experts Opinion. *Cardiovasc Intervent Radiol*. 2016;39(3):334–343.
15. Hong K, Khwaja A, Liapi E, Torbenson MS, Georgiades CS, Geschwind J-FH. New intra-arterial drug delivery system for the treatment of liver cancer:

- preclinical assessment in a rabbit model of liver cancer. *Clin Cancer Res.* 2006;12(8):2563–2567.
16. Gnutzmann DM, Mechel J, Schmitz A, et al. Evaluation of the plasmatic and parenchymal elution kinetics of two different irinotecan-loaded drug-eluting embolics in a pig model. *J Vasc Interv Radiol.* 2015;26(5):746–754.
 17. Saxena A, Bester L, Shan L, et al. A systematic review on the safety and efficacy of yttrium-90 radioembolization for unresectable, chemorefractory colorectal cancer liver metastases. *J Cancer Res Clin Oncol.* 2014;140(4):537–547.
 18. Poston GJ, Figueras J, Giuliante F, et al. Urgent Need for a New Staging System in Advanced Colorectal Cancer. *J Clin Oncol.* 2017;26(29):4828–4833.
 19. Gennari L, Doci R, Bozzetti F, Veronesi U. Proposal for a clinical classification of liver metastases. *Tumori.* 1982;68(5):443–449.
 20. Fortner JG, Silva JS, Golbey RB, Cox EB, Maclean BJ. Multivariate analysis of a personal series of 247 consecutive patients with liver metastases from colorectal cancer. I. Treatment by hepatic resection. *Ann Surg.* 1984;199(3):306–316.
 21. Petrelli NJ, Bonnhaim DC, Herrera LO, Mittelman A. A proposed classification system for liver metastasis from colorectal carcinoma. *Dis Colon Rectum.* 1984;27(4):249–252.
 22. Gayowski TJ, Iwatsuki S, Madariaga JR, et al. Experience in hepatic resection for metastatic colorectal cancer: analysis of clinical and pathologic risk factors. *Surgery.* 1994;116(4):703-10-1.
 23. Nordlinger B, Guiguet M, Vaillant JC, et al. Surgical resection of colorectal carcinoma metastases to the liver. A prognostic scoring system to improve case selection, based on 1568 patients. *Association Française de Chirurgie. Cancer.* 1996;77(7):1254–1262.
 24. Eisenhauer EA, Therasse P, Bogaerts J, et al. New response evaluation criteria in solid tumours: revised RECIST guideline (version 1.1). *Eur J Cancer.* 2009;45(2):228–247.
 25. Janne d’Othée B, Sofocleous CT, Hanna N, et al. Development of a research agenda for the management of metastatic colorectal cancer: proceedings from a multidisciplinary research consensus panel. *J Vasc Interv Radiol.* 2012;23(2):153–163.
 26. Gonzalez-Guindalini FD, Botelho MPF, Harmath CB, et al. Assessment of liver tumor response to therapy: role of quantitative imaging. *Radiographics.* 2013;33(6):1781–1800.
 27. Lin M, Pellerin O, Bhagat N, et al. Quantitative and volumetric European association for the study of the liver and response evaluation criteria in solid tumors measurements: Feasibility of a semiautomated software method to assess tumor response after transcatheter arterial chemoembolization. *J Vasc Interv Radiol.* 2012;23(12):1629–1637.
 28. Chapiro J, Duran R, Lin M, et al. Early survival prediction after intra-arterial therapies: a 3D quantitative MRI assessment of tumour response after TACE or radioembolization of colorectal cancer metastases to the liver. *Eur Radiol.* 2015;25(7):1993–2003.
 29. Sahu S, Scherthaner R, Ardon R, et al. Imaging Biomarkers of Tumor Response in Neuroendocrine Liver Metastases Treated with Transarterial

- Chemoembolization: Can Enhancing Tumor Burden of the Whole Liver Help Predict Patient Survival? *Radiology*. 2016;0(0):160838.
30. Tacher V, Lin M, Duran R, et al. Comparison of Existing Response Criteria in Patients with Hepatocellular Carcinoma Treated with Transarterial Chemoembolization Using a 3D Quantitative Approach. *Radiology*. 2016;278(1):275–284.
 31. Fleckenstein FN, Scherthaner RE, Duran R, et al. 3D Quantitative tumour burden analysis in patients with hepatocellular carcinoma before TACE: comparing single-lesion vs. multi-lesion imaging biomarkers as predictors of patient survival. *Eur Radiol*. 2016;26(9):3243–3252.
 32. Chapiro J, Duran R, Lin M, et al. Identifying Staging Markers for Hepatocellular Carcinoma before Transarterial Chemoembolization: Comparison of Three-dimensional Quantitative versus Non-three-dimensional Imaging Markers. *Radiology*. 2015;275(2):438–447.
 33. Namasivayam S, Martin DR, Saini S. Imaging of liver metastases: MRI. *Cancer Imaging*. 2007;7:2–9.
 34. Bonekamp D, Bonekamp S, Halappa VG, et al. Interobserver agreement of semi-automated and manual measurements of functional MRI metrics of treatment response in hepatocellular carcinoma. *Eur J Radiol*. 2014;83(3):487–496.
 35. Tacher V, Lin M, Chao M, et al. Semiautomatic Volumetric Tumor Segmentation for Hepatocellular Carcinoma. *Acad Radiol*. 2013;20(4):446–452.
 36. Chapiro J, Wood LD, Lin M, et al. Radiologic-pathologic analysis of contrast-enhanced and diffusion-weighted MR imaging in patients with HCC after TACE: diagnostic accuracy of 3D quantitative image analysis. *Radiology*. 2014;273(3):746–758.
 37. Pellerin O, Lin M, Bhagat N, Ardon R, Mory B, Geschwind J-F. Comparison of Semi-automatic Volumetric VX2 Hepatic Tumor Segmentation from Cone Beam CT and Multi-detector CT with Histology in Rabbit Models. *Acad Radiol*. 2013;20(1):115–121.
 38. Papademetris X, Jackowski MP, Rajeevan N, et al. BioImage Suite: An integrated medical image analysis suite: An update. *Insight J*. 2006;2006:209.
 39. Kim S, Mannelli L, Hajdu CH, et al. Hepatocellular carcinoma: Assessment of response to transarterial chemoembolization with image subtraction. *J Magn Reson Imaging*. 2010;31(2):348–355.
 40. Contal C, O’Quigley J. An application of changepoint methods in studying the effect of age on survival in breast cancer. *Comput Stat Data Anal*. 1999;30(3):253–270.
 41. Bradburn MJ, Clark TG, Love SB, Altman DG. Survival Analysis Part III: Multivariate data analysis – choosing a model and assessing its adequacy and fit. *Br J Cancer*. 2003;89(4):605–611.
 42. Lencioni R, Llovet JM. Modified RECIST (mRECIST) assessment for hepatocellular carcinoma. *Semin Liver Dis*. 2010;30(1):52–60.
 43. Van Cutsem E, Cervantes A, Nordlinger B, Arnold D. Metastatic colorectal cancer: ESMO Clinical Practice Guidelines for diagnosis, treatment and follow-up. *Ann Oncol*. 2014;25(suppl_3):iii1-iii9.
 44. Edwards MS, Chadda SD, Zhao Z, Barber BL, Sykes DP. A systematic review of

- treatment guidelines for metastatic colorectal cancer. *Colorectal Dis.* 2012;14(2):e31-47.
45. Abdalla EK, Vauthey J-N, Ellis LM, et al. Recurrence and outcomes following hepatic resection, radiofrequency ablation, and combined resection/ablation for colorectal liver metastases. *Ann Surg.* 2004;239(6):818-25-7.
 46. Forner A, Reig M, Bruix J. Hepatocellular carcinoma. *Lancet (London, England).* 2018;391(10127):1301–1314.
 47. Kanematsu M, Kondo H, Goshima S, et al. Imaging liver metastases: review and update. *Eur J Radiol.* 2006;58(2):217–228.
 48. Juntu J, Sijbers J, Dyck D, Gielen J. Bias Field Correction for MRI Images. *Comput Recognit Syst.* 2005. p. 543–551.
 49. Yazdani S, Yusof R, Riazi A, Karimian A. Magnetic resonance image tissue classification using an automatic method. *Diagn Pathol.* 2014;9:207.
 50. Knijn N, Mekenkamp LJM, Klomp M, et al. KRAS mutation analysis: A comparison between primary tumours and matched liver metastases in 305 colorectal cancer patients. *Br J Cancer.* 2011;104(6):1020–1026.